Eur. Phys. J. D **5**, 167–171 (1999)

THE EUROPEAN PHYSICAL JOURNAL D

EDP Sciences

Calculation of the contributions from high-n dielectronic satellites to the Kα resonance line in helium-like iron

J.-G. Wang[1,3,a], T.-Q. Chang[1], C.-Z. Dong[2], and T. Kato[3]

[1] Institute of Applied Physics and Computational Mathematics, P.O. Box 8009, Beijing 100088, P.R. China
[2] Department of Physics, Northwest Normal University, Lanzhou 730070, P.R. China
[3] National Institute for Fusion Science, Oroshi-cho, Toki, Gifu, 509-5292, Japan

Received: 16 April 1998 / Revised: 8 September 1998 / Accepted: 14 September 1998

Abstract. A simplified relativistic configuration interaction method is used to study the dielectronic satellite transition processes. In this method, the infinite resonant doubly excited states can be calculated, and furthermore, the whole high-n dielectronic satellite transition processes can be treated conveniently by interpolation (rather than extrapolation) in the frame of Quantum Defect Theory. As an example, we calculate the contributions from high-n dielectronic satellites to the $K\alpha$ resonance line in helium-like iron, and the results are in good agreement with the experimental measurements.

PACS. 34.80.Kw Electron-ion scattering; excitation and ionization – 34.80.Dp Atomic excitation and ionization by electron impact

1 Introduction

The $K\alpha$ X-ray emission of the transition metals Ti, Cr, Fe, and Ni is extensively used for determining the parameters of high-temperature tokamak plasmas [1–6]. But it is blended with lithiumlike dielectronic satellites due to transitions $1s^2nl-1s2pnl$ with $n \geq 3$. These unresolved satellites lead to a significant increase in both the apparent width and intensity of the resonance line which must be taken into account for Doppler-broadening and Doppler-shift measurements, as well as for the evaluation of the satellite-to-resonance-line ratio which is used for diagnostics of solar flares and tokamak plasmas [6–12]. In these important diagnostic applications, it is necessary to determine the contribution of these satellites as accurately as possible. In plasma, due to blending with the resonance line, their intensities and positions have never been measured directly and reliance must be solely on theory. However, explicit calculations of the high-n-satellite line strengths are difficult because the number of resonance doubly excited states increases rapidly with the principal quantum number of the outermost occupied shell of the resonance state; there even exist infinite resonance doubly excited states which emit the high-n-satellite lines as the principal quantum number of the outermost occupied shell approaches infinity. As a result, most of the explicit calculations have been limited so far to low-lying resonance doubly excited states with $n \leq 4$, while an approximate $1/n^3$ scaling law has generally been used to extrapolate the satellite intensity factors for $n > 4$ [1,13–17]. But for low Z or low ionization stage ions, due to strong screening, the extrapolation is not reliable [18]. Karim and Bhalla have performed explicit calculations of $n = 3 - 8$ dielectronic satellite line strengths using the Hartree-Fock atomic model for helium-like Ne, Si, Ar, Ti, Cr, and Ni, and check the validity of the $1/n^3$ scaling law approximately [19]. In fact, Quantum Defect Theory (QDT) has been developed to treat the atomic processes involving high Rydberg states [20–22], and this was also used to study the DR cross-sections and rate coefficients for high Rydberg states by extrapolation [18,23–26]. Recently, in the frame of QDT, we have developed a simplified relativistic configuration interaction (SRCI) method to study the dielectronic recombination (DR) processes. In this method, all the resonant doubly excited high Rydberg states can be treated in an unified manner by interpolation (rather than extrapolation), and then the DR cross-sections and rate coefficients can be obtained conveniently. We have calculated the DR cross-sections of the hydrogen-like and helium-like ions [27–31] and the results are in agreement with the experimental measurement [32–34].

In the present paper, a similar method is developed to calculate the contributions from high-n dielectronic satellite (DS) lines to the resonance line, in which all the high-n dielectronic satellites involving infinite resonant doubly excited states can be calculated conveniently by interpolation in the frame of QDT. As an example, we study the contributions from high-n DS lines to the $K\alpha$ resonance line in helium-like iron, and the theoretical results are compared with the experimental measurements.

[a] e-mail: wang@nifs.ac.jp

2 Theoretical method

The DS transition processes of helium-like iron has the form

$$e^- + \mathrm{Fe}^{24+}(1s^2) \rightarrow \mathrm{Fe}^{23+}(1sn_rl_rnl)^{**} \rightarrow \mathrm{Fe}^{23+}(1s^2nl)^* + h\nu. \quad (1)$$

Here, as a free electron with a specific kinetic energy collides with an iron ion $\mathrm{Fe}^{24+}(1s^2)$ (denoted by i), one bound electron of $\mathrm{Fe}^{24+}(1s^2)$ is excited from $1s$ orbital into n_rl_r orbital and the free electron is captured into an unoccupied orbital nl, and then a resonant doubly excited state $\mathrm{Fe}^{23+}(1sn_rl_rnl)^{**}(j)$ is formed; subsequently, the resonant doubly excited state decays into a non-autoionizing state $\mathrm{Fe}^{23+}(1s^2nl)^*(k)$ through radiative transition processes $\mathrm{Fe}^{23+}(1sn_rl_rnl)^{**} \rightarrow \mathrm{Fe}^{23+}(1s^2nl)^*$, which emits the di-electronic satellite line.

The total DS cross-section from i to j and finally to k can be obtained in the isolated resonances approximation (atomic units are used throughout unless specified),

$$\sigma_{DS}(i,j,k) = \sigma^c_{i,j}B^r_{j,k} \quad (2)$$

where $\sigma^c_{i,j}$ is the cross-section of the resonance capture processes, in which the Fe^{24+} ion in initial state $i(1s^2)$ captures a free electron with a specific energy ϵ_i and forms the resonance doubly excited state $j(1sn_rl_rnl)$. $B^r_{j,k}$ is the radiative branching ratio from state j to the final state k. $\sigma^c_{i,j}$ and $B^r_{j,k}$ can be calculated by

$$\sigma^c_{i,j} = \frac{\pi^2\hbar^3}{m_e\epsilon_i}\frac{g_j}{2g_i}A^a_{j,i}\delta(\epsilon-\epsilon_i), \quad (3)$$

and

$$B^r_{j,k} = \frac{A^a_{j,k}}{\sum_{k'}A^r_{j,k'} + \sum_{i'}A^a_{j,i'}} \quad (4)$$

where g_i and g_j are the statistical weight of the state i and j, respectively. The summation i' is over all possible Auger final states of Fe^{23+} (j), and the summation k' is over all possible states of Fe^{23+} whose energies are below state j. $\delta(\epsilon-\epsilon_i)$ is a delta function. A^a_{ji} $(A^a_{ji'})$ is Auger decay rate (inverse resonant capture), which can be calculated by the Fermi golden rule,

$$A^a_{ji} = \frac{2\pi}{\hbar}|\langle\Psi_j|\sum_{s<t}\frac{1}{r_{s,t}}|\Psi_{i\epsilon_i}\rangle|^2, \quad (5)$$

where Ψ_j and $\Psi_{i\epsilon_i}$ are antisymmetrized many-electron wavefunctions for j state and i state plus a free electron, respectively.

We construct the configuration wavefunctions $\phi(\Gamma JM)$ (Γ denotes the quantum numbers $1sn_rl_rnl$ and parity) as anti-symmetrized product-type wavefunctions from central-field Dirac orbitals with appropriate angular momentum coupling [35]. All relativistic single-electron wavefunctions (bound and continuum) are calculated based on the atomic self-consistent potential [36,37]. An atomic state function for the state $j(1sn_rl_rnl)$ with total angular momentum JM is then expressed as linear superposition of the configuration wavefunctions with same principal quantum numbers (n_r, n), and same orbital angular momentum quantum numbers (l_r, l)

$$\psi_j(JM) = \sum_{\lambda=1}^{m} C_{j\lambda}\phi(\Gamma_\lambda JM). \quad (6)$$

Here m is the number of the configuration wavefunctions and the mixing coefficients $C_{j\lambda}$ for state j are obtained by diagonalizing the relevant Hamiltonian matrices [35]. The free state is chosen as the single configuration wavefunction. Then we have

$$A^a_{ji} = \frac{2\pi}{\hbar}|\sum_{\lambda=1}^{m}C_{j\lambda}M^a_{ij\lambda}|^2, \quad (7)$$

where the Auger decay matrix element $M^a_{ij\lambda}$ is defined as

$$M^a_{ij\lambda} = \langle\phi(\Gamma_\lambda JM)|\sum_{s<t}\frac{1}{r_{s,t}}|\Psi_{i\epsilon_i}\rangle. \quad (8)$$

Based on QDT, when (n_r,l_r,l) are fixed and n varies from bound to continuum state, all the resonant doubly excited states with same J will form a channel. In the channel, the energy-normalized matrix element can be defined as

$$\overline{M}^a_{ij\lambda} = M^a_{ij\lambda}(\nu_n^{3/2}/q), \quad (9)$$

here (ν_n^3/q^2) is the density of states [29,30], $\nu_n = n - \mu_n$, and μ_n is the corresponding quantum defect. This energy-normalized matrix element $\overline{M}^a_{ij\lambda}$ varies smoothly with the electron orbital energy in the channel. When the energy-normalized matrix elements of a few states (including one continuum state) in a channel have been calculated, the Auger decay matrix elements of infinite discrete states of that channel can be obtained by interpolation [29]. On the other hand, the mixing coefficients $C_{j\lambda}$ in (6) are almost unchanged within a channel [29]. We can use the mixing coefficients of a state with a certain high principal quantum number to approximate that of those states with higher principal quantum number. From the expression (7), the Auger rates and capture rates (by detailed balance) of the infinite resonant doubly excited states can be obtained conveniently.

A^r_{jk} is radiative decay rate, which is defined as

$$A^r_{jk} = \frac{4e^2\omega}{3\hbar c^3 g_j}|\langle\Psi_j|T^{(1)}|\Psi_k\rangle|^2, \quad (10)$$

where ω is photon energy, $T^{(1)}$ is electronic dipole operator [35]. The atomic wavefunction Ψ_k for final state k can be constructed in the similar way as the expression (6)

$$\psi_k(J'M') = \sum_{\lambda'=1}^{m'}C_{k\lambda'}\phi'(\Gamma'_\lambda J'M'). \quad (11)$$

Then we have

$$A^r_{jk} = \frac{4e^2\omega}{3\hbar c^3 g_j} |\sum_{\lambda,\lambda'=1}^{m,m'} C_{j\lambda} C_{k\lambda'} M^r_{jk}|^2, \qquad (12)$$

where the radiative transition matrix element is defined as

$$M^r_{jk} = \langle \phi(\Gamma_\lambda JM)|T^{(1)}|\phi'(\Gamma'_\lambda J'M')\rangle. \qquad (13)$$

For the radiative process with the final state $k(1s^2nl)$, the resonant doubly excited states with the fixed angular momentum character $(n_r l_r, l)$ and different orbital energy form a channel. In the channel, the energy-normalized radiative transition matrix element is defined as

$$\overline{M}^r_{jk} = M^r_{jk}(\nu_n^{3/2}/q). \qquad (14)$$

This energy-normalized matrix element varies slowly with the electron orbital energy. By interpolation, all the energy-normalized matrix elements of infinite discrete states in a channel can be obtained [29]. From the expression (12), we can obtain all the radiative rates in the channel.

The resonance energy ϵ_i can be calculated under the frozen core approximation [38]. Then, we can obtain the DS cross-sections in formula (2) for any resonant doubly excited states conveniently.

The DS strength, which is the integral of the DS cross-section over the resonance energy width, can be written as

$$S_{ijk} = \frac{\pi^2\hbar^3}{m_e\epsilon_j}\frac{g_j}{2g_i}\frac{A^a_{ji}A^r_{jk}}{\sum_{k'}A^r_{jk'} + \sum_{i'}A^a_{ji'}}. \qquad (15)$$

Then, the calculated cross-sections should be convoluted with a Gaussian distribution of an energy resolution Γ. Here, the experimental resolution width 50 eV (FWHM) is used.

The convoluted cross-section is

$$\sigma^{DS}_t(\epsilon) = \sum_j \frac{S_{ijk}}{\sqrt{2\pi}\Gamma}\exp\left[-\frac{(\epsilon-\epsilon_j)^2}{2\Gamma^2}\right]. \qquad (16)$$

We also present the spectral contribution of different high-n DS lines, in which the DS strengths are convoluted with a Gaussian distribution of an experimental wavelength resolution $\Delta\lambda/\lambda = 1/3600$,

$$\sigma^{DS}_\lambda(\lambda) = \sum_j \frac{S_{ijk}}{\sqrt{2\pi}\Delta\lambda}\exp\left[-\frac{(\lambda-\lambda_{jk})^2}{2\Delta\lambda^2}\right]. \qquad (17)$$

Here λ_{jk} is the DS wavelength, whose separation from the resonance line $K\alpha$ is given in Figure 2.

3 Results and discussion

As an example, we study the contributions from high-n dielectronic satellites to the $K\alpha$ resonance lines in helium-like iron. The convoluted cross-section as a function of free electron energy is given in Figure 1a. The resolved features correspond to the emission from the KLM ($n = 3$), KLN ($n = 4$) and KLO ($n = 5$) resonances and the high-n contribution is calculated by the QDT. The strength of each resonance decreases as n increases; however, the number of resonances in a given interval increases, and the convoluted cross-section therefore varies smoothly across the threshold for electron-impact excitation. The relevant experimental intensities of the $K\alpha$ radiation is given in Figure 1b [10]. Our calculated positions and relative intensities of each of the resonances are in agreement with the experimental measurements.

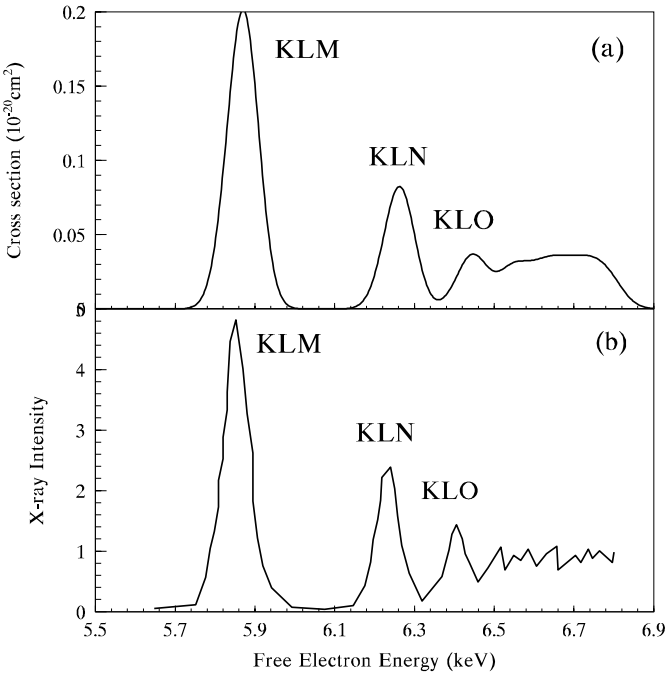

Fig. 1. (a) Calculated DS cross-sections as a function of electron energy for the $n = 3, 4, 5, \ldots \infty$ resonances; (b) experimental DS intensities below threshold for electron-impact excitation [10].

Table 1. The DS resonance strengths for $n = 3, 4, 5$ and $n \geq 6$.

Resonance	Total S_{cal} (10^{-20} cm^2 eV)	Total S_{exp} [10] (10^{-20} cm^2 eV)
$n = 3$	28.14	30.92
$n = 4$	11.18	10.32
$n = 5$	4.83	4.50
$n \geq 6$	11.89	11.36

Our calculated DS strengths are given in Table 1. It can be seen that although the strength of each resonance decreases as n increases, the resonances ($n > 3$) almost give the same contribution as the resonances ($n = 3$); even the resonances $n \geq 6$ (in our calculation, we choose $n \leq 50$) also give an important contribution. Our calculated spectral contribution of different high-n DS lines as the separation from the $K\alpha$ resonance line is shown in

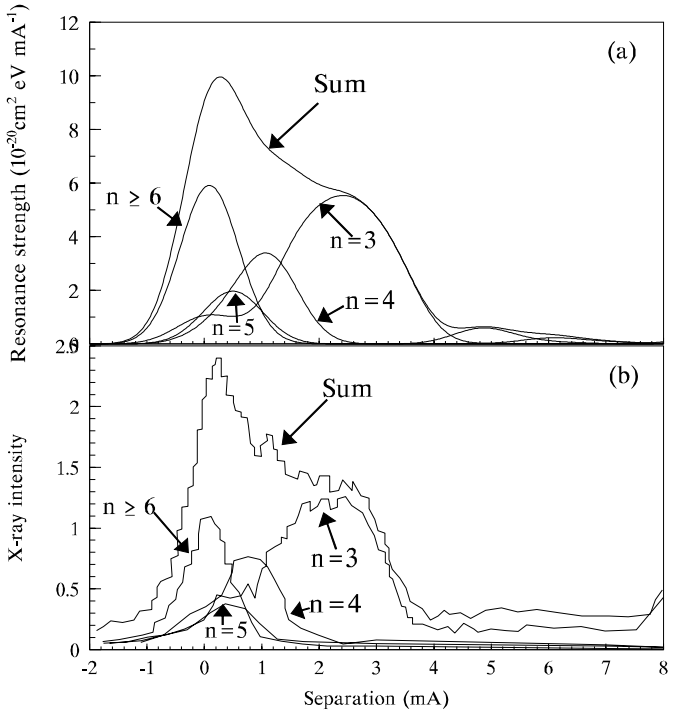

Fig. 2. (a) Calculated DS cross-sections as a function of separation from $K\alpha$ resonance line for the $n = 3, 4, 5, \ldots \infty$ resonances; (b) experimental DS intensities [10].

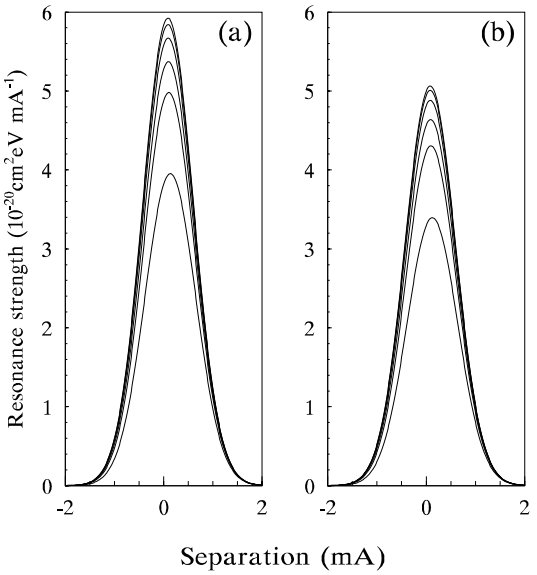

Fig. 3. (a) DS cross-sections by the SRCI method as a function of separation from $K\alpha$ resonance line for the $n = 6$ to n_{max} resonances, the curves (down to up) correspond to $n_{max} = 10$, 15, 20, 30, 50, 100, respectively; (b) DS cross-sections on n^{-3} extrapolation as a function of separation from $K\alpha$ resonance line for the $n = 6$ to n_{max} resonances, the curves (down to up) are corresponding to $n_{max} = 10$, 15, 20, 30, 50, 100, respectively.

Figure 2a, which are compared with the relative experimental values in Figure 2b [10]. The comparison shows our results are in good agreement with the experimental measurements of positions and relative strength. We can see that the high-n satellites are found mostly on the long wavelength side, and their position approaches the resonance line as the n increases. This means that these high-n DS lines are seriously mixed with resonance lines, such as the resonances with $n \geq 6$ in Figure 2, and it is very difficult to separate them through experiments. In the practical diagnostic application, it only can rely on theoretical calculations to treat these high-n contributions. In previous works [1,13–17], an approximate $1/n^3$ scaling law has generally been used to extrapolate the satellite intensity factors for high n resonances. But for low Z or low ionization stage ions, the satellite intensity factors don't have a good n^{-3} scaling relation. The reason is the following: it is well-known that only when $A^r \gg A^a$, we have

$$\sigma^{DS} \propto \frac{A^a_{ji} \sum_k A^r_{jk}}{\sum_{k'} A^r_{jk'} + \sum_{i'} A^a_{ji'}} \sim \sum_k A^a_{ji} \sim n^{-3}.$$

However, generally for low Z ions or low ionization stage ions, the relation $A^r \gg A^a$ can not be satisfied. Even though the relation is satisfied, due to the strong screening, the scaling relation $A^a_{ji} \sim n^{-3}$ needs to be revised [18]. In our SRCI method, after the renormalized matrix elements of a few benchmark points (several bound points and one continuum point) have been calculated, we can obtain all the DS strength in a channel by interpolation.

In Figure 3, the results for high n resonances $n \geq 6$ of SRCI method are compared with that of n^{-3} extrapolation from our data $n = 4$, and the extrapolation is the same as the references [1,13–17]. The contributions $6 \leq n \leq n_{max}$ in different maximum n_{max} ($n_{max} = 10, 15, 20, 30, 50, 100$) are also displayed in Figure 3. In order to determine the total high-n contribution, we must decide the maximum principal quantum number n_{max} for doubly excited states. In the EBIT experiment [10], all the resonances until the collision excitation threshold have been measured. So we think it almost included all the high-n contributions, we choose $n_{max} = 50$ in our calculation. If we choose a small n_{max}, for example, $n_{max} = 10$, we will underestimate the high-n contributions ($n \geq 6$) by about 25%, and the agreement in Table 1 for $n \geq 6$ resonances can not be preserved. The contribution from resonances $n > 50$ is only a few percent of that from $6 \leq n < 50$, which can be neglected. In the practical diagnostic application, the n_{max} depends on the plasma conditions, such as plasma temperature and density. Using a simple method to estimate the n_{max} [39], we can obtain the $n_{max} > 100$ when the plasma density is 10^{14} cm^{-3} and temperature is 100 eV for Fe^{23+}. As the plasma density decreases and temperature increases, the n_{max} increases [39]. So high-n contributions should be considered in laboratory or astrophysical plasma. Comparing Figures 3a and 3b, the n^{-3} extrapolation for the satellite density factor underestimates the high n contributions ($n \geq 6$) about 15% percent, and the n^{-3} extrapolation should be improved for high n resonances.

Finally, we would like to conclude by making the following comments. In the present paper, a simplified relativistic configuration interaction method is used to study the dielectronic satellite transition processes. In this method, the important contribution of high-n dielectronic satellite lines can be treated conveniently by interpolation in the frame of Quantum Defect Theory. It is essential for practical diagnostic application, because the higher the principal quantum number of dielectronic satellite lines is, the stronger the blending of dielectronic satellite lines with resonance lines. Due to the relativistic treatment, our SRCI method should be applicable especially for high Z ions.

This work was partly supported by National Science Foundation of China, Pos. Doc. Foundation of China, Youth Foundation of Chinese High Tech., and the Japan Society for Promotion of Science.

References

1. F. Bely-Dubau, A.H. Gabriel, S. Volonte, Mon. Not. R. Astron. Soc. **189**, 801 (1979).
2. J. Dubau, A.H. Gabriel, M. Loulergue, L. Steenman-Clark, S. Volonte, Mon. Not. R. Astron. Soc. **195**, 705 (1981).
3. M. Bitter, S. von Goeler, K.W. Hill, R. Horton, D. Johnson, W. Roney, N.R. Sauthoff, E. Silver, W. Stodiek, Phys. Rev. Lett. **47**, 921 (1981).
4. F. Bely-Dubau, P. Faucher, L. Steenman-Clark, M. Bitter, S. von Goeler, K.W. Hill, C. Camhy-Val, J. Dubau, Phys. Rev. A **26**, 3549 (1982).
5. M. Bitter, K.W. Hill, M. Zarnstorff, S. von Goeler, R. Hulse, L.C. Johnson, N.R. Sauthoff, S. Sesnic, K.M. Young, M. Tavernier, F. Bely-Dubau, P. Faucher, M. Cornille, J. Dubau, Phys. Rev. A **32**, 3011 (1985).
6. V. Decaux, M. Bitter, H. Hsuan, K.W. Hill, S. von Goeler, H. Park, C.P. Bhalla, Phys. Rev. A **44**, R6987 (1991).
7. M. Bitter, K.W. Hill, N.R. Sauthoff, P.C. Efthimion, E. Meservey, W. Roney, S. von Goeler, R. Horton, M. Goldman, W. Stodiek, Phys. Rev. Lett. **43**, 129 (1979).
8. U. Feldman, G.A. Doschek, R.W. Kreplin, Astrophys. J. **238**, 365 (1980).
9. K. Tanaka, T. Watanabe, K. Nishi, K. Akita, Astrophys. J. **254**, L59 (1982).
10. P. Beiersdorfer, M.B. Schneider, M. Bitter, S. von Goeler, Rev. Sci. Instrum. **63**, 5029 (1992).
11. T. Kato, Phys. Scripta T **73**, 98 (1997).
12. T. Kato, T. Fujiwara, Y. Hanaoka, Astrophys. J. **492**, 822 (1998).
13. F. Bely-Dubau, A.H. Gabriel, S. Volonte, Mon. Not. R. Astron. Soc. **186**, 405 (1979).
14. C.P. Bhalla, K.R. Karim, Phys. Rev. A **34**, 3525 (1986), C.P. Bhalla, K.R. Karim, T. Reeves, Phys. Scripta **34**, 747 (1986).
15. J. Nilsen, At. Data Nucl. Data Tab. **37**, 191 (1987); *ibid.* **38**, 339 (1988).
16. M.H. Chen, At. Data Nucl. Data Tab. **34**, 101 (1986); Phys. Rev. A **38**, 3230 (1988).
17. F. Bombarda, R. Giannella, E. Kallne, G.J. Tallents, F. Bely-Dubau, P. Faucher, M. Cornille, J. Dubau, A.H. Gabriel, Phys. Rev. A **37**, 504 (1988).
18. Y. Hahn, Adv. At. Mol. Phys. **21**, 123 (1985).
19. K.R. Karim, C.P. Bhalla, Phys. Rev. A **43**, 615 (1991).
20. M. Gailitis, Sov. Phys.-JETP **17**, 1328 (1963).
21. U. Fano, J. Opt. Soc. Am. **65**, 979 (1975).
22. M.J. Seaton, Proc. Phys. Soc. Lond. **88**, 801 (1966); Rep. Prog. Phys. **46**, 167 (1983).
23. J. Dubau, J. Wells, J. Phys. B **2**, 1452 (1973).
24. M.J. Seaton, P.J. Storey, in *Atomic processes and applications*, edited by P.G. Burke, B.L. Moiseiwitsch (North-Holland Publishing Company, 1976), p. 133.
25. J. Dubau, S. Volonte, Rep. Prog. Phys. **43**, 167 (1980).
26. R.H. Bell, M.J. Seaton, J. Phys. B, At. Mol. Phys. **18**, 1589 (1985).
27. Chen-zhong Dong, Yu Zou, Jian-Guo Wang, Jia-Ming Li, Acta Phys. Sin. **44**, 1712 (1995).
28. Jian-Guo Wang, Yu Zou, Chen-Zhong Dong, Jia-Ming Li, Chin. Phys. Lett. **12**, 530 (1995).
29. Jian-Guo Wang, Yi-zhi Qu, Jia-Ming Li, Phys. Rev. A **52**, 4274 (1995).
30. Yi-zhi Qu, Jian-Guo Wang, Jian-Kui Yuan, Jia-Ming Li, Phys. Rev. A **57**, 1033 (1998).
31. Jian-Guo Wang, Tie-Qiang Chang, Yi-Zhi Qu, Eur. Phys. J. D **2**, 231 (1998).
32. D.R. DeWitt, D. Schneider, M.W. Clark, M.H. Chen, Phys. Rev. A **44**, 7185 (1991).
33. D.R. DeWitt, R. Schuch, T. Quinteros, H. Gao, W. Zong, H. Danared, M. Pajek, N.R. Badnell, Phys. Rev. A **50**, 1257 (1994).
34. G. Kilgus, D. Habs, D. Schwalm, A. Wolf, R. Schuch, N.R. Badnell, Phys. Rev. A **47**, 4859 (1993).
35. Zhong-Xin Zhao, Jia-Ming Li, Acta Phys. Sin. **34**, 1469 (1985).
36. Jia-Ming Li, Zhong-Xing Zhao, Acta Phys. Sin. **34**, 97 (1982).
37. D.A. Liberman, D.T. Cromer, J.T. Waber, Comput. Phys. Commun. **2**, 107 (1971).
38. C.M. Lee, Jia-Ming Li, Phys. Rev. A **10**, 584 (1974).
39. H.R. Griem, *Principles of Plasma Spectroscopy* (Cambridge University press, 1997).